In Situ Field Emission of Density-Controlled ZnO Nanowire Arrays**

By *Xudong Wang*, *Jun Zhou*, *Changshi Lao*, *Jinhui Song*, *Ningsheng Xu*, and *Zhong L. Wang**

Owing to their unique semiconducting properties, ZnO nanowires (NWs) have received intensive research interests in optics,[1,2] electronics,[3,4] piezoelectrics,[5] and mechanics.[6] The vertically aligned morphology has already shown great advantages in manipulation and device assembly within the nanometer regime.[7–10] Among them, field emission (FE) is one of the most important applications since the emitting efficiency can be highly improved by the alignment.[11,12] Comprehensive theoretical and experimental research on FE has been mainly conducted on carbon nanotubes (CNTs) owing to their good conductivity, chemical stability, and easy as well as cost-effective fabrication.[13,14] It has been discovered that the emitter density is very critical to the emission efficiency.[15–17] An array of densely packed CNTs greatly reduces the field-enhancement factor at the CNT tip to a level not much different from a flat metal plate. Too loosely distributed CNTs cannot meet the desired requirement of high current density and high-emitting points. Oxide semiconducting NWs, which are more stable at high temperatures in an oxygen environment and have a more controllable electronic property, have been considered more and more as alternative FE sources instead of CNTs. With a large exciton binding energy and high melting temperature, ZnO NWs have recently been studied as an effective FE source.[18–21] However, very little research has been performed on optimizing their FE property by controlling the density of the aligned ZnO NWs. Recently, we developed a low-cost self-assembly process to synthesize aligned ZnO NWs with controlled sizes, lengths, and densities.[22,23] Moreover, with the simultaneous formation of a continuous conductive layer at the roots, these NW arrays exhibit great merit for device applications, such as FE.

In a FE measurement, the distance between the sample and counter electrode is an important parameter to determine the field-enhancement factor. However, this distance is usually difficult to precisely determine inside a vacuum-testing chamber. In order to perform an accurate investigation, we developed an in situ measuring system inside a scanning electron microscope chamber, in which the emitting distance could be directly observed. The working vacuum of the chamber at ca. 5×10^{-6} Torr (1 Torr = 133.322 Pa) provides a reasonable vacuum condition for emission testing. This system provided a novel and reliable way to measure the FE property with knowledge of the exact emitting distance, nanowire density, and the region being tested. In this paper, we report such in situ measurements on a series of aligned ZnO NWs with controlled density and size. It was found that the NWs with a density between 60 and 80 μm^{-2} and a length of ca. 1 μm gave the highest emitting current, which was ca. 20 μA at a field of 10 V μm, detected by using a 0.03 mm^2 W counter electrode.

The setup of the in situ measuring system is schematically shown in Figure 1a and detailed information is presented in

[*] Prof. Z. L. Wang, Dr. X. D. Wang, J. Zhou, C. S. Lao, J. H. Song
School of Materials Science and Engineering
Georgia Institute of Technology
Atlanta, GA 30332-0245 (USA)
E-mail: zhong.wang@mse.gatech.edu
J. Zhou, Prof. N. S. Xu
School of Physics and Engineering
State Key Lab of Optoelectronic Materials and Technologies
SunYat-Sen (Zhongshan) University
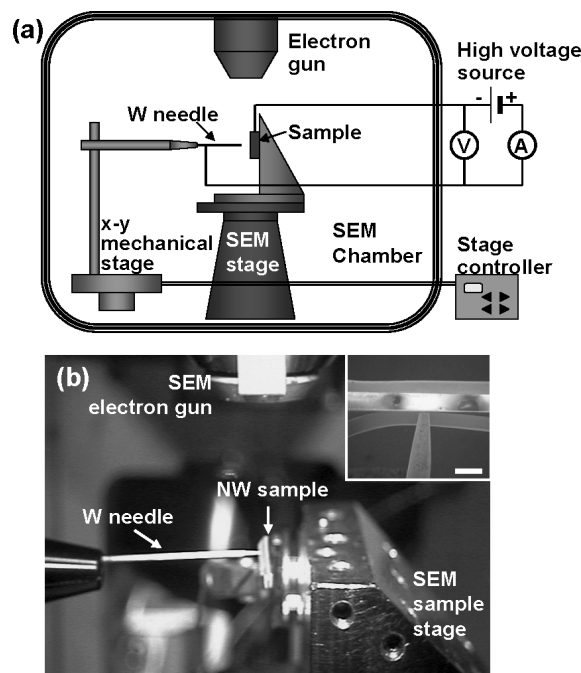Guangzhou, 510275 (P.R. China)

Figure 1. Setup of the scanning electron microscope in situ FE measurement system. a) Schematic of the setup. b) Photo of the system inside the scanning electron microscope chamber; inset: a scanning electron microscopy (SEM) image of the W needle tip pointing to the nanowire arrays, the scale bar represents 500 μm.

the Experimental section. Figure 1b shows an optical photo of the scanning electron microscope chamber equipped with this in situ measuring system. Before the measurement, the W needle and the NWs had to be aligned under the electron beam so that the scanning electron mircoscope could see both of them. Since the x–y mechanical stage had a lower movement resolution, the W needle was located first until the flat tip was observed at the center of the microscope's imaging screen. Then, the NW sample was moved towards the W tip, and focusing both of them by the electron beam at the same time guaranteed that they were aligned at the same height, as shown in the inset of Figure 1b.

The typical morphology of the density-controlled aligned ZnO NWs is shown in the scanning electron microscopy (SEM) image in Figure 2a. This shows the NW sample with the highest density (ca. 110 μm^{-2}). Every single NW was self-aligned perpendicular to the substrate and there was no bend-
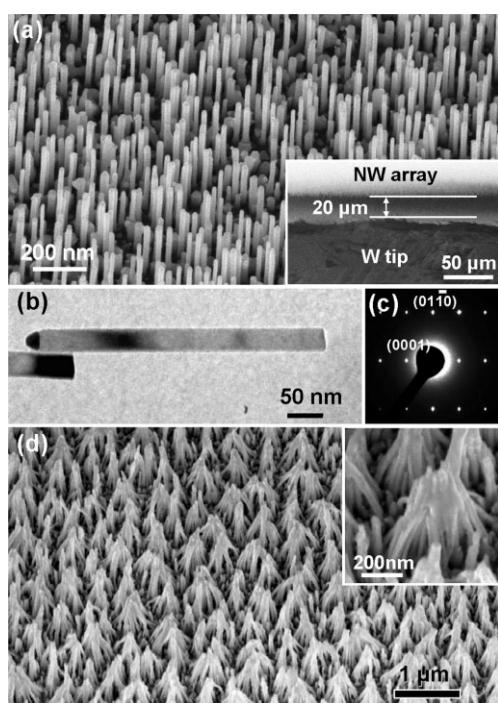

Figure 2. a) A representative SEM image of aligned ZnO NWs; inset: an SEM image of the FE testing condition. b) A transmission electron microscopy (TEM) image of a typical ZnO nanowire. c) A corresponding electron diffraction pattern. d) An SEM image of the highest density ZnO NWs after FE testing; inset: an enlarged SEM image of one nanowire bundle.

ing or interconnects between the NWs, which make them a perfect sample for a FE property study. The length of the NWs varied from ca. 0.7 to 1 μm and their widths were ca. 30–40 nm, as shown in the transmission electron microscopy (TEM) image in Figure 2b. A ca. 10–20 nm gold particle could be observed at the tip of most of the NWs. All of the NWs were single crystalline and their growth direction was along the [0001] direction (Fig. 2c).

During the in situ FE measurement, the vacuum of the scanning electron microscope chamber was at ca. 5×10^{-6} Torr. The distance between the NW array and the W tip was controlled by fine movement of the scanning electron microscope stage and measured directly from the SEM image, as shown in the inset of Figure 2a. This distance was kept at 20 μm for all of the measurements. The NWs were also examined by using SEM after FE tests. Most of the gold catalyst tips were gone after several electron emission steps. Notably, after the emission, the highest density NWs were attracted together to form bundles, as shown in Figure 2d. This was possibly due to the potential-induced self-attracting effect,[24] upon the application of a high voltage. On the other hand, the magnetic field created by one stream of FE current by a few NWs would create an attractive Lorentz force for the next stream of NWs, similar to the self-attraction of two parallel conducting wires. Moreover, during the emission, the Joule heating effect sintered them and some of them eventually merged together (inset of Fig. 2d). This phenomenon was not found for aligned NW arrays with lower densities.

The FE property was measured on the aligned ZnO NWs with five different densities. All of them were grown on the same substrate and measured one after the other under the exact same conditions.[18] Typical top-view SEM images of the five samples are shown in Figure 3a, where they are identified from I to V with a density of 108, 86, 64, 45 and 28 NWs/μm^{-2}, respectively. The FE I–V curves are shown in Figure 3b. The counter electrode (the W needle tip) has an area of only 0.03 mm^2, which was much smaller than the size of the sample. However, considering the density of the aligned NWs, the number of NWs covered under the counter electrode was of the order of 10^6 to 10^7, which is big enough to show a representative universal property. Therefore, the total current received was determined by the size of the W tip so that the measured emission current for samples of different grown areas can be compared directly. Similar to CNTs, the highest density NWs did not prove to be a very effective emission source (the curve composed by diamond dots). The emission was turned on by the electric field around 20 V μm^{-1} and the emission current increased to ca. 20 μA when the electric field ramped up to 25 V μm^{-1}. This was believed to be caused by a screening effect due to the very small space between the NWs. However, from the SEM observation, the agglomeration of the NWs largely reduced the sharp emitting tips. Therefore, in this case, the self-attracting phenomenon in high-density NWs would also be responsible for their low emission efficiency.

The highest emission efficiency was observed on samples II and III, which had medium densities (86 and 64 μm^{-2}) and are marked by triangles and crosses, respectively, in Figure 3b. Their turn-on electric field was 8–10 V μm^{-1} and the emission current sharply jumped up to ca. 20 μA at a field of 10–13 V μm^{-1}. When the NW density was decreased to 45 μm^{-2} and lower, the emission efficiency became very low, as shown by the star and circle points in Figure 3b. Their highest emission current only reached 1–2 μA under an electric field of 25 V μm^{-1} (500 V).
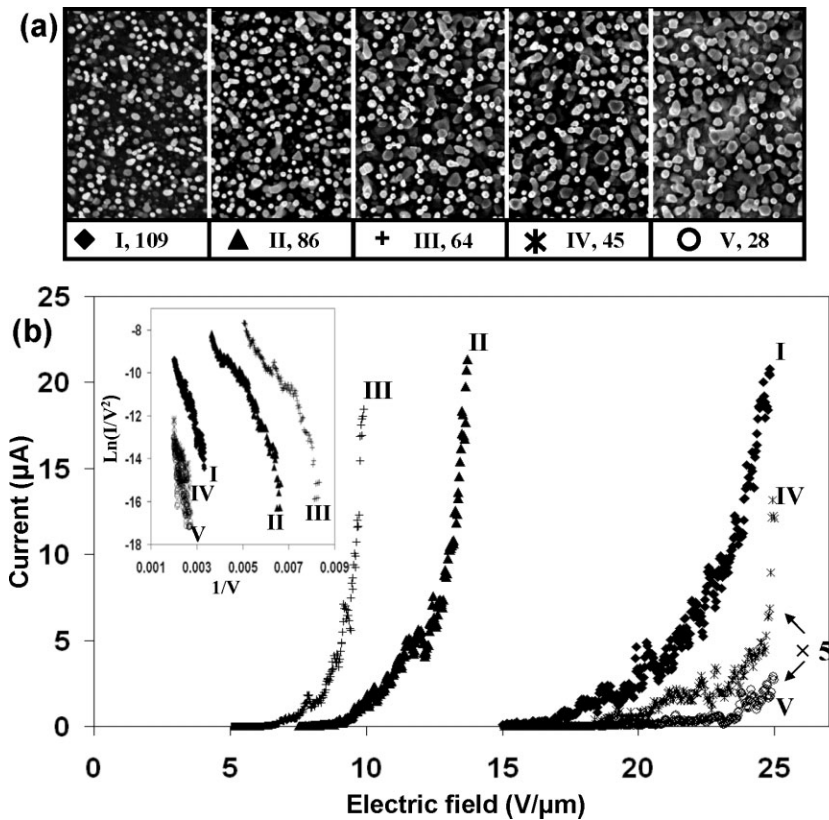
Figure 3. a) Top-view SEM images of the aligned ZnO nanowire arrays with five different densities (NWs/µm^{-2}). Curves IV and V are magnified five times for better illustration. b) Corresponding FE *I–V* characteristics and the converted F–N curves.

The emission *I–V* curves were converted by using the Fowler–Nordheim (F–N) equation and plotted as ln(I/V^2) versus 1/V, as shown in the inset of Figure 3b. The five curves exhibited almost straight lines and the field-enhancement factors (β) were calculated from the slopes (k_{F-N}) according to the equation

$$k = B\phi^{3/2}d/\beta \tag{1}$$

where φ is the work function of ZnO, *d* is the emitting distance, and $B = 6.83 \times 10^9 \ \text{V}\,\text{eV}^{-3/2}\,\text{m}^{-1}$. By taking 5.2 eV as a fixed work-function value for ZnO NWs[25] and keeping the distance at 20 µm, the field-enhancement factors were calculated and listed in Table 1. In the CNT model presented by Nilsson et al.,[15] the distance between the emitters was the key parameter that determines the field-enhancement factor. In our case, we estimated the average distance between the NWs by assuming that they were evenly distributed on the substrate. The best field-enhancement factor of aligned ZnO NWs was found to be >800, which is a reasonable value for the application as an electron-emitting source. Thus, the optimum interspacing of ZnO NWs should be 110–130 nm, which is about 10 times smaller than the theoretical calculation for CNTs.[16] The value of β dramatically dropped when the inter-

spacing increased to 150 nm. The small number of emitting tips (NWs) on the substrate was generally considered as the reason for this low emitting ability. However, for the low-density NW arrays, there were many gold/ZnO particles left on the substrate during the growth. The electric-field distribution around the NW tips would be disturbed by the neighboring particles so that the field-enhancement factors were further reduced.[26]

In reality, the NW distributions were very random, while the theoretical prediction was based on a uniform arrangement. It is necessary to reveal how close our assumption is to the real cases. Therefore, additional FE tests were performed on a patterned ZnO NW array with almost the same density as the unpatterned low-density NWs. Both samples are shown in Figure 4a. Obviously, the distance between the NWs in the patterned sample was much more uniform than the unpatterned one. Moreover, since the density was controlled by the prepatterned catalyst dots, no redundant gold particles were left on the substrate, while in the unpatterned sample, a lot of gold/ZnO particles can be found lying around the NWs. The corresponding FE *I–V* characteristics and their F–N curves are shown in Figure 4b. The patterned sample showed a low turn-on electric field at ca. 9 V µm^{-1}, which was less than half of that given by the unpatterned sample (ca. 21 V µm^{-1}). Both F–N curves exhibited an almost linear shape. From their slopes, the field-enhancement factors were calculated and are listed in Table 2, where the β of the patterned sample was 716, almost two times larger than the unpatterned sample. This high emitting efficiency of the patterned NWs was attributed to the uniform NW distribution and the clean substrate. First, NWs in the unpatterned sample were unevenly distributed, especially for the low-density ones. As shown in the right-hand-side image of Figure 4a, several NWs grew very close together but were far away from the others. So, the screening effect still applied on those NWs and reduced the emitting efficiency. On the other hand, the

Table 1. Summary of the field-enhancement factors of ZnO NWs with different densities.

Sample	NW density [µm^{-2}]	Average distance between NWs [nm]	k_{F-N}	β
I	109	96	−3252	498
II	86	108	−2019	802
III	64	125	−1883	860
IV	45	150	−4371	370
V	28	190	−5185	312

(a)

◆ density: ~30 μm⁻² — 400 μm   ▲ density: ~32 μm⁻² — 300 μm
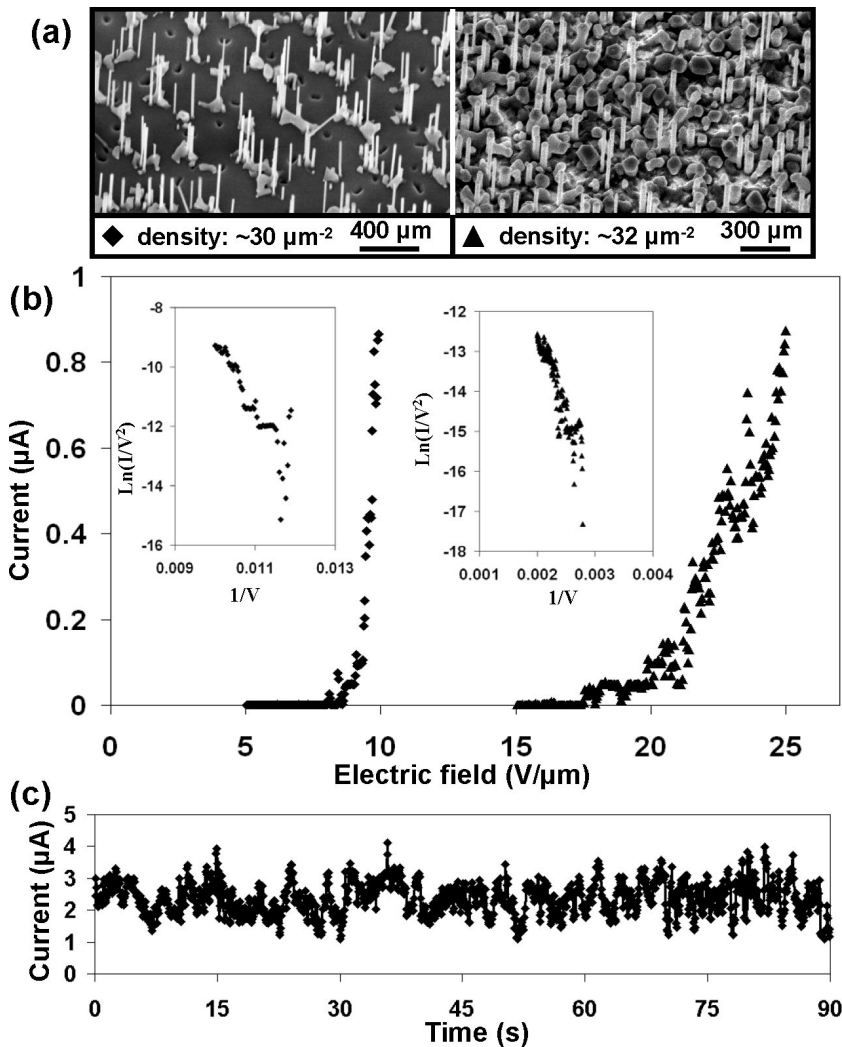
(b)

(c)

Figure 4. a) SEM images of patterned (left) and unpatterned (right) ZnO NWs with very close densities. b) Corresponding FE *I–V* characteristics and the converted F–N curves. c) Emission current of the patterned ZnO NWs showing the stability.

Table 2. Summary of the field-enhancement factors of patterned/unpatterned ZnO NWs.

Sample	NW density [μm⁻²]	Average distance between NWs [nm]	$k_{F–N}$	β
Patterned	30	182	−2262	716
Unpatterned	32	177	−3879	417

large gold particles would disturb the electric-field distribution during FE. Therefore, the evenly distributed aligned NWs without disturbance from other metal particles would give a much higher emitting efficiency.

A FE stability measurement was performed on the patterned ZnO NW sample by keeping the electric field at $12 \, V \, \mu m^{-1}$. The emission current was recorded for 90 s, as shown in Figure 4c. The current was fluctuated between 2 to $4 \, \mu A$ and steadily remained in this region during the entire measurement.

In summary, by setting up a second stage inside a scanning electron microscope chamber, we developed an effective in situ FE measurement system, where the distance between the emitting source and counter electrode could be accurately measured and finely controlled. In such a system, we characterized the FE property of the aligned ZnO NWs with different densities. It was found that the NWs with a density between 60 and 80 μm⁻² and of ca. 1 μm in length gave the highest emitting current. Moreover, a uniform distribution of NWs and a clean/flat substrate could further increase the emitting efficiency. The reasonably high field-enhancement factor and the stability measurement suggest that the aligned ZnO NWs could be an effective and reliable electron-emitting source.

Experimental

Density-controlled aligned ZnO NWs were grown on an expitaxial layer of AlGaN coated on a *c*-plane orientated sapphire substrate. The density was controlled by varying the thickness of the gold catalyst from 1 to 8 nm on a 1 cm × 2 cm substrate [23]. The growth of ZnO NWs was through a vapor–solid–liquid (VLS) process [27]. In general, a mixture of equal amounts (by weight) of ZnO and graphite powders were used as source materials and loaded in an alumina boat, which was located at the center of an alumina tube. Ar mixed with 2 % O_2 was used as the carrier gas at a total flow rate of 50 sccm. The substrate was placed down stream in a temperature zone of ca. 850 °C. A horizontal tube furnace was used to heat the center of the alumina tube to 950 °C at a rate of $50 °C \, min^{-1}$, and the temperature was held at the peak temperature for 30 min under a pressure of 30 mbar. After the growth, the system was slowly cooled down to room temperature under the flow of the mixing carrier gas.

The in situ measuring system was set up inside a LEO 1530 FE SEM chamber. As schematically shown in Figure 1a, under the electron gun, the NW sample was perpendicularly mounted on a cliff side of a triangular-shaped scanning electron microscope sample holder, which was attached to the SEM stage with a moving resolution of a few nanometers. A W needle with a flat top was used as the counter electrode and held by a stainless steel mini post system. In order to achieve independent movements of the W electrode, the post system was attached to another *x–y* movement stage (ca. 20 nm moving resolution) that was screwed on the side of the SEM stage. This *x–y* stage was controlled by an outside controller through the electronic interface built on the door of the scanning electron microscope chamber. Meanwhile, the NW sample and the W needle were connected to the negative and positive electrodes, respectively, of an outside high DC voltage source. The voltage was read out by the meter on the voltage source and the current was measured by using a pico-ampere meter.

[1] Q. X. Zhao, M. Willander, R. E. Morjan, Q. H. Hu, E. E. E. Campbell, *Appl. Phys. Lett.* **2003**, *83*, 165.

[2] X. D. Wang, C. Neff, E. Graugnard, Y. Ding, J. S. King, L. A. Pranger, R. Tannenbaum, Z. L. Wang, C. J. Summers, *Adv. Mater.* **2005**, *17*, 2103.

[3] M. Arnold, P. Avouris, Z. W. Pan, Z. L. Wang, *J. Phys. Chem. B* **2003**, *107*, 659.

[4] B. A. Buchine, W. L. Hughes, F. L. Degertekin, Z. L. Wang, *Nano Lett.* **2006**, *6*, 1155.

[5] Z. L. Wang, J. H. Song, *Science* **2006**, *312*, 242.

[6] J. H. Song, X. D. Wang, E. Riedo, Z. L. Wang, *Nano Lett.* **2005**, *5*, 1954.

[7] M. Huang, S. Mao, H. Feick, H. Yan, Y. Wu, H. Kind, E. Weber, R. Russo, P. Yang, *Science* **2001**, *292*, 1897.

[8] M. Law, L. E. Greene, J. C. Johnson, R. Saykally, P. Yang, *Nat. Mater.* **2005**, *4*, 455.

[9] X. D. Wang, C. J. Summers, Z. L. Wang, *Nano Lett.* **2004**, *4*, 423.

[10] W. I. Park, G. C. Yi, *Adv. Mater.* **2004**, *16*, 87.

[11] Q. Zhao, H. Z. Zhang, Y. W. Zhu, S. Q. Feng, X. C. Sun, J. Xu, D. P. Yua, *Appl. Phys. Lett.* **2005**, *86*, 203 115.

[12] G. Shen, Y. Bando, B. Liu, D. Golberg, C.-J. Lee, *Adv. Funct. Mater.* **2006**, *16*, 410.

[13] W. A. de Heer, A. Chatelain, D. Ugarte, *Science* **1995**, *270*, 1197.

[14] S. Fan, M. G. Chapline, N. R. Franklin, T. W. Tombler, A. M. Cassell, H. Dai, *Science* **1999**, *283*, 512.

[15] L. Nilsson, O. Groening, C. Emmenegger, O. Kuettel, E. Schaller, L. Schlapbach, *Appl. Phys. Lett.* **2000**, *76*, 2071.

[16] J. M. Bonard, N. Weiss, H. Kind, T. Stöckli, L. S. Forró, K. Kern, A. Châtelain, *Adv. Mater.* **2001**, *13*, 184.

[17] K. B. K. Teo, M. Chhowalla, G. A. J. Amaratunga, W. I. Milne, G. Pirio, P. Legagneux, F. Wyczisk, D. Pribat, D. G. Hasko, *Appl. Phys. Lett.* **2002**, *80*, 2011.

[18] C. J. Lee, T. J. Lee, S. C. Lyu, Y. Zhang, H. Ruh, H. J. Lee, *Appl. Phys. Lett.* **2002**, *81*, 3648.

[19] Y. W. Zhu, H. Z. Zhang, X. C. Sun, S. Q. Feng, J. Xu, Q. Zhao, B. Xiang, R. M. Wang, D. P. Yu, *Appl. Phys. Lett.* **2003**, *83*, 144.

[20] S. H. Jo, J. Y. Lao, Z. F. Ren, R. A. Farrer, T. Baldacchini, J. T. Fourkas, *Appl. Phys. Lett.* **2003**, *83*, 4821.

[21] D. Banerjee, S. H. Jo, Z. F. Ren, *Adv. Mater.* **2004**, *16*, 2028.

[22] J. H. Song, X. D. Wang, E. Riedo, Z. L. Wang, *J. Phys. Chem. B* **2005**, *109*, 9869.

[23] X. D. Wang, J. H. Song, C. J. Summers, J. H. Ryou, P. Li, R. D. Dupuis, Z. L. Wang, *J. Phys. Chem. B* **2006**, *110*, 7720.

[24] X. D. Wang, C. J. Summers, Z. L. Wang, *Appl. Phys. Lett.* **2005**, *86*, 013 111.

[25] X. D. Bai, E. G. Wang, P. X. Gao, Z. L. Wang, *Nano Lett.* **2003**, *3*, 1147.

[26] Z. Xu, X. D. Bai, E. G. Wang, Z. L. Wang, *J. Phys.: Condens. Matter* **2005**, *17*, L507.

[27] X. D. Wang, J. H. Song, P. Li, J. H. Ryou, R. D. Dupuis, C. J. Summers, Z. L. Wang, *J. Am. Chem. Soc.* **2005**, *127*, 7920.